Ion heating and energy redistribution in a collisionless shock wave

N. A. Strokin

Siberian Institute of Terrestrial Magnetism, Ionosphere, and Radiowave Propagation
(Submitted 18 January 1985)
Zh. Eksp. Teor. Fiz. **88**, 2005–2014 (June 1985)

Results are reported of a laboratory study of the evolution of the ion-energy spectrum across a magnetoacoustic collisionless shock wave (CSW) with Alfven-Mach number in the range $1.6 \lesssim M_A \lesssim 6.1$. Ions reflected by the CSW were recorded in the entire range of values of M_A. Combined analysis of measurements in laboratory, terrestrial, and interplanetary CSW's has shown that the ion-ion interaction on the wave front ensures most of the dissipation of the energy of directed motion of the plasma flow. It results in the heating of the core of the distribution function for small M_S and M_A (M_S is the ion-acoustic Mach number) and the increase in the relative number of reflected ions due to the reduction in the directed velocity on scattering in the ion-ion interaction zone, i.e., for large M_S and M_A. The intermediate values of M_S, M_A between these two regimes, determined from the change in the shape of the reflected particle distribution (plateau → beam) and the reduction in the ion temperature behind the CSW are: M_S 03.5–4, $M_A \approx 3$.

INTRODUCTION

The relatively few laboratory experiments on the characteristics of the ion component of plasmas in transverse collisionless shock waves (CSW) during the first "golden decade"[1] of CSW studies (1964–1974)[2–6] and during the next decade[7,8] resulted in the following qualitative CSW picture in "ion light." Throughout the investigated range of the values of the Mach–Alfven number $M_A = U/V_A$ (U is the CSW velocity, $V_A = H_0/(4\pi n_0 m_i)^{1/2}$ is the Alfven velocity, n_0, H_0 are, respectively, the initial concentration of plasma and the magnetic field, and m_i is the ion mass), the ion energy distribution is non-Maxwellian: there is a low-energy core, shifted by the amount equal to the directed energy of the CSW, and a high-energy tail extending[2–5,7,8] to a few keV. The temperature T_{i2} of core ions behind the wave front can reach a few tens of eV, and increases[5] with increasing M_A. The presence of high-energy particles is explained by the reflection of some of the incident plasma currents from the discontinuity in the potential φ_2 on the wave front.[4,7,8] Ions are reflected from the CSW, beginning with $M_A \approx M_{c1}$ (M_{c1} is the first critical number, $M_A \approx 3$), and the relative number of reflected particles, n_{refl}/n_0, increases[6] with increasing M_A. The high-energy part of the distribution function may be either of the beam type or it can take the form of a plateau.[8]

A large volume of experimental data was obtained in recent years on the ion parameters, using artificial earth satellites and space probes to examine CSW's in the Earth's vicinity and in interstellar space (see, for example, Refs. 1 and 9–14).

The ion energy spectra are non-Maxwellian with a well-defined core throughout the range of solar-wind parameters that have been investigated. Moreover, this shape of the distribution function appears ahead of the CSW front, persists in the front, and extends well behind it. The high-energy part of the proton spectrum is considered to be due to specular and nonspecular reflection of incident solar-wind particles from the CSW. The structure of the distribution tail is made up of beams of reflected and gyrorotating particles. The density of the reflected ions ranges from 1–3% of the solar-wind density for $M_A \approx 2$ to 15–20% for $M_A = 8$–12 (Ref. 13). Electron thermalization occurs up to the ion-heating region.[10]

The currently available extensive set of parameters measured simultaneously over the wave front now provides the basis for a deeper investigation of the mechanisms responsible for the dissipation of directed CSW energy. By comparing the spectra and intensity of the lower hybrid plasma oscillations with the ion energy spectra, it has been shown[12] that the main mechanism of dissipation for CSW with $M_A = 10$ in the Earth's neighborhood may be the ion-ion instability in a transverse magnetic field.

Analysis of satellite data was based on conclusions derived from laboratory CSW studies. On the one hand, we used the ideas and the developed theory of the CSW, and on the other hand, a model-based analogy of properties. The possibility and limitations of this analogy were justified and defined in Refs. 15–18. The most reliable analogy in qualitative (restricted) simulation is possible when a phenomenon is physically modeled as a whole. This requires, at the very least, that the conditions for the existence of physical processes responsible for the given phenomenon are satisfied. In the case of the collisionless shock wave (in the presence of an ultrasonic plasma flow and a magnetic barrier), these involve the collective particle interaction, each with its own excitation (saturation) threshold. Thus, model analogy implies, firstly, that the excitation thresholds for processes governing the phenomenon both in space and in the laboratory have been exceeded and, secondly, that they are identical. Comparison of the range of processes recorded at present in terrestrial, interplanetary, and laboratory transverse CSW's has led to the conclusion that the basic properties of all these shock waves are identical, so that model analogy is justified, as is the combined analysis of all the results, aimed at gathering new knowledge.

CSW studies have not as yet provided an unambiguous answer to the question: what is the mechanism governing the

 0038-5646/85/061187-06$04.00

heating of the bulk of the ions and the redistribution of the energy of directed CSW motion? The variation in the ion energy spectra with varying initial conditions has not been examined either.

In this paper, the combined analysis of laboratory data on the ion energy distribution in a transverse CSW and an analysis of previously published data on terrestrial and interplanetary quasiperpendicular CSW are used to show that the heating and reflection of ions is largely the result of a collective process, namely, the ion-ion interaction. The reflected-particle distribution function changes its shape (plateau → beam) as we pass through $M_S \approx 3.5$–4 (M_S is the ion-acoustic Mach number) and $M_A \approx 3$. The temperature T_{i2} is found to fall with increasing M_S, M_A during this process, and both n_{refl}/n_0 and the total energy E_{col} received by the ions as a result of the collective interaction (i.e., the thermal energy of the core and beam ions, which are small in comparison with the thermal energy of the core ions, plus the kinetic energy of directed motion of the reflected particles) are found to increase.

LABORATORY SETUP AND DIAGNOSTIC METHODS

The experiments were performed on the theta-pinch system "UN-Phoenix."[19,8] Hydrogen plasma with n_0 and H_0 in the region in which a detached shock wave was formed (zone II in Fig. 1; Ref. 8) was first produced in a cylindrical glass chamber with an internal diameter of 15 cm. The plasma was compressed by a magnetic piston with an amplitude $H_1 \simeq 1200$ Oe and rise time $\tau \simeq 400$ ns. The mass number range employed was $1.6 \lesssim M_A \lesssim 6.1$. The reflected ions were unmagnetized ($t \lesssim \omega_{Hi}^{-1}$, where t is the lifetime of the CSW and $\omega_{Hi} = eH_0/m_i c$). The initial temperature was[8] $T_0 \simeq T_{i0} \simeq T_{e0} \simeq 1$–2 eV. The initial concentration was monitored by interferometry ($\lambda = 2$ mm, 4 mm). The radial distribution of the magnetic field and the CSW propagation velocity were recorded in the central section of the shock coil, using two open-loop magnetic probes (3 mm in diameter) located at 3 and 4.5 cm from the axis, respectively. The potential φ_2 was measured by a floating electric probe ($R_3 = 12$ kΩ) at the same radial distances.[8]

The ion-energy spectrum was deduced from the energy distribution of neutral charge-transfer particles[20] emitted by the plasma. The measurements were performed in the energy range 140–1840 eV, using an eight-channel netural-particle energy analyzer with a time resolution $\Delta t = 13$–3.6 ns and energy resolution $\Delta E/E = 30$–3% (channels 1–8, respectively).[21] The neutral particles were extracted from the working volume via a ceramic tube with an internal diameter of 5 mm and mounted along the radius of the vacuum chamber in the central section of the shock coil. The tube was shifted from the axis of the system by 1.3 cm in order to exclude effects occurring during the final stage of the collapse of the cylindrical current shell. The procedure used to construct the spectra is similar to that in Ref. 22.

EXPERIMENTAL RESULTS

Signals from the analyzer detectors are recorded in the form of one or two peaks, 50–150 ns long, separated by intervals of 30–100 ns, depending on the initial conditions. The first peak corresponds to an instant of time at which the CSW has not yet reached the entrance tube of the analyzer and the second of the instant at which the wave emerges

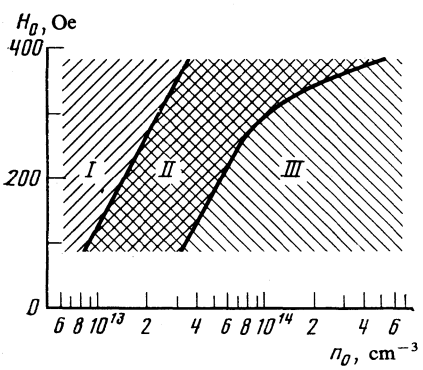

FIG. 1. Propagation of a magnetic disturbance: I—diffusive penetration of magnetic fields; II—existence of detached CSW; III—existence of reflecting piston.

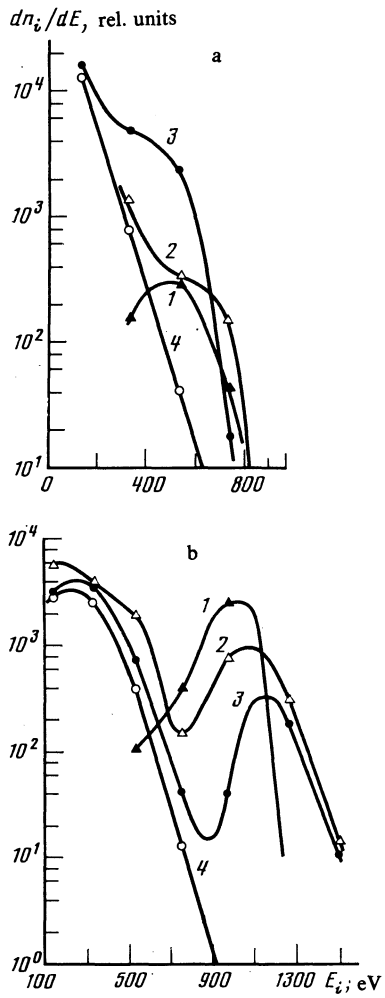

FIG. 2. Typical ion energy distributions for small M_A (a—$H_0 = 380$ Oe, $n_0 = 8 \times 10^{13}$ cm^{-3}, $M_A = 2.1$, $M_S = 3.1$) and large M_A (b—$H_0 = 160$ Oe, $n_0 = 3 \times 10^{13}$ cm^{-3}, $M_A = 3.6$, $M_S = 4.5$).

from the tube. In addition to this "two-period" modulation, each peak may, in turn, consist of a number of "elementary" peaks, the intensity maxima of which are separated by 10–40 ns. A variety of proton energy spectra is observed, depending on this complex signal structure and the varying relative positions of signals in different channels of the instrument. Typical distributions for small ($\lesssim 3$) and large M_A are shown in Fig. 2.

Ions that have overtaken the CSW are observed immediately ahead of the front. Most of them have energies satisfying the relation $E_{\text{refl}} \approx m_i(u+V)^2/2$, where E_{refl} is the energy of ions reflected from the potential jump φ_2 propagating with velocity U and $V_\varphi = (2e\varphi_2/m_i)^{1/2}$; some of them are particles with thermal velocities $V_{Ti} > U$ (see Fig. 2, curve 1). Curves 2 and 3 in Fig. 2 refer to the interior of the CSW front. The time interval between them is 25–30 ns. For small M_A, the reflected-particle beam has the relaxed form and, as the point with maximum amplitude of the magnetic field H_2 in the CSW front is approached (curve 3, Fig. 2a), the energy of directed motion of the beam is reduced. For a shock wave with large M_A, the ion energy distribution retains the beam shape across the entire width of the front (Refs. 2 and 3 in Fig. 2b).

Reflected particles are observed at all points on the magnetic profile and in the region immediately behind it, which extends over 20–30 ns. Spectra recorded outside the region in which the reflected particles are recorded, i.e., behind the CSW front (curve 4 in Fig. 2), have a Maxwellian shape (straight lines on the semilogarithmic scale). These distributions were subsequently used to determine the ion temperature T_{i2} behind the shock-wave front.

Figure 3 (curve 1) shows T_{i2} as a function of M_A. Despite the considerable spread of the experimental points, it may be concluded that T_{i2} decreases with increasing M_A, reaching values of about 20 eV for $M_A \simeq 5$. The important characteristic of shock waves is the efficiency ζ with which the directed motion of the shock wave is converted into the heating of ions: $\zeta = 2T_{i2}/m_iU^2$. The function $\zeta = f(M_A)$ is plotted in Fig. 4 (curve 1). By analogy with the function $T_{i2} = \varphi(M_A)$, this curve is also found to fall with increasing M_A.

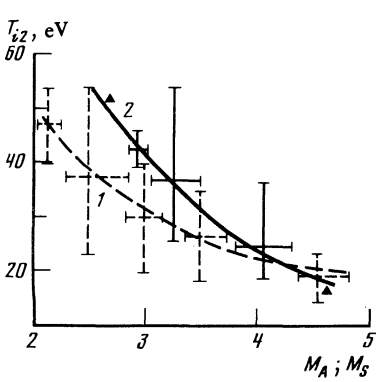

FIG. 3. Ion temperature behind the CSW front as a function of M_A (curve 1) and M_S (curve 2). The points are experimental.

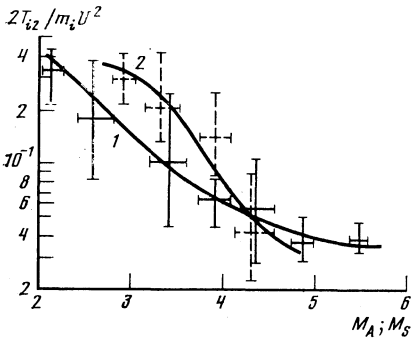

FIG. 4. Efficiency of conversion of the energy of directed motion of the CSW, $\zeta = 2T_{i2}/m_iU^2$, into ion heating as a function of M_A (curve 1) and M_S (curve 2).

The recorded T_{i2}, especially for small M_A, exceed the heating by both the adiabatic compression ($\lesssim 8$ eV) and the speeding up of ions in the region of the ion-acoustic current instability (5–10 eV).[23]

The fact that the CSW front contains ion currents moving with relative velocity $V_d = (2e\varphi_2/m_i)^{1/2}$ in the entire range of initial parameters that was investigated, suggests that short-wave ion-Langmuir and ion-acoustic oscillations[24,25,27] could be excited on the scale of the front as a result of the ion-ion instability. The character of the ineraction between the ion currents is strongly dependent on the ratio V_d/C_S [$C_S = (T_e/m_i)^{1/2}$ is the velocity of ion sound and T_e is the electron temperature]. When $V_d/C_s \lesssim 3$, the beam excites oscillations mostly along $\mathbf{V}_d$ and is therefore effectively retarded, thus heating the main current. When $V_d/C_s \gg 3$, the oscillations are almost perpendicular to $\mathbf{V}_d$ and this leads to the scattering of the beam without loss of energy. The two processes occur simultaneously in the intermediate region.[27] It was therefore decided to investigate T_{i2} and ζ as functions of $V_d/C_{S2} = M_S$, where $C_{S2} = (T_{e2}/m_i)^{1/2}$ and T_{e2} is the maximum electron temperature in the CSW (at the point corresponding to the maximum amplitudes of H_2 and φ_2, and immediately behind the front). No account was taken in the calculation of C_{S2} of the heating of ions by the ion-acoustic current instability in the CSW front, so that our values of M_S are actually overestimated. The quantity T_{e2} was determined in this experiment from the measured values of H_0, n_0, and $h = (H_2 - H_0)/H_2$, using the graph of $4\pi nT_{e2}/H_0^2 = \phi(h)$ given in Fig. 2 of Ref. 32 (n is the particle density behind the CSW front and $n \approx hn_0$). This has enabled us to construct approximate graphs of T_{i2} and ζ as functions of M_S (curve 2 in Figs. 3 and 4, respectively) and of M_S as a function of M_A (Fig. 5, curve 1). When the value $M_S = 3.5$–4 was exceeded, the parameters T_{i2} and ζ decreased sufficiently rapidly whilst M_S increased with increasing M_A.

Analysis of the shape of the distribution functions for different values of M_S calculated as above shows that the spectra with the relaxed beam and high T_{i2} are obtained for lower M_S (in Fig. 2a, $M_S \simeq 3.1$). The beam distributions and the lower T_{i2} are characteristic for regimes with high M_S (in Fig. 2b, $M_S \simeq 4.5$). The values $M_S \simeq 3.5$–4 and $M_A \simeq 3$ are

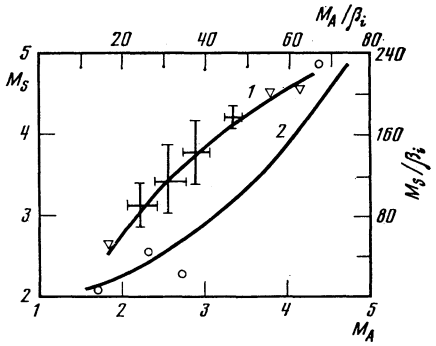

FIG. 5. M_S as a function of M_A (curve 1) and M_S/β_i as a function of M_A/β_i (curve 2).

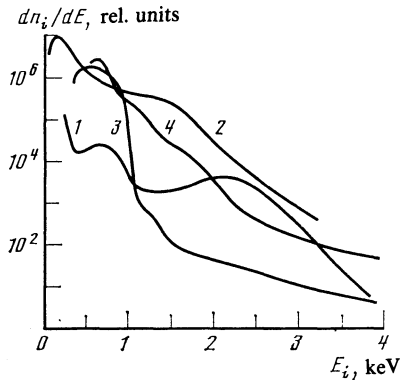

FIG. 6. Ion energy distribution (ISEE-II sattelite): curve 1—proton energy spectrum behind the CSW front near the Earth on 27 August 1978, 20:08:00 UT; 2—ditto for 7 November 1977, 22:52:13 UT; 3—energy spectrum of protons ahead of the interplanetary CSW front on 13 November 1979, 07:34:03 UT; 4—proton energy spectrum behind the interplanetary CSW front on 30 November 1979, 07:38:12 UT.

intermediate in the sense that they correspond to the transition region between the ion interaction regimes.

RESULTS OF REDUCTION OF SATELLITE DATA

We have used published data[10,13,14,26,28] on quasiperpendicular shock waves. The one-dimensional[11] and two-dimensional[13,14,26,28] proton velocity distributions were first converted into energy distributions, where, for the original data in two-dimensional velocity space, we constructed the energy spectra both in the direction of motion of the main body of the plasma current and in the instantaneous directions of motion of the beams of gyrorotating ions. The temperature T_{i2} of the bulk of the protons (core of the distribution function) was determined from the segment of the energy spectrum lying outside the E_{refl} region, approximated by the isotropic Maxwellian distribution and shifted by an amount equal to the directed energy found from the $f(V)$ and $f(V, \phi)$ curves, where ϕ is the angle in the plane of the ecliptic between the plasma velocity vector and the direction of the sun. The remaining plasma parameters were taken from published values of $\theta_{\mathbf{Vn}}$ and time profiles of T_e, n_e, B, $\theta_{\mathbf{Bn}}$ (B is the magnetic field, $\theta_{\mathbf{Bn}}$ is the angle between the normal $\mathbf{n}$ to the CSW front and the interplanetary magnetic field vector, $\theta_{\mathbf{Vn}}$ is the angle between $\mathbf{n}$ and the velocity of solar wind $\mathbf{V}_{SW}$, and n_e is the electron density). The relative velocity of the ion current, V_d, was determined from the $f(V, \phi)$ profiles by algebraic composition of the velocities of the main plasma current and of the groups of gyrorotating ions at different points on the CSW front.

The data reduced refer to the period of low-velocity solar wind ($V_{SW} \lesssim 4.2 \times 10^7$ cm/s), for which the initial proton energy distribution at distances ~ 1 AU (AU is the astronomical unit) is practically the isotropic Maxwellian distribution with $T_{i\parallel} \simeq T_{i\perp} = 5$–$10$ eV ($T_{i\parallel}$, $T_{i\perp}$ are the proton temperatures along and at right-angles to the interplanetary magnetic field). An enhanced concentration of high-energy particles in the solar wind was not observed under these conditions, at least, at a level of intensity lower by three orders of magnitude than the intensity of protons moving with V_{SW} (Ref. 28).

Several factors indicate the necessity of taking into account the ion-ion interaction in the above events. All the energy spectra constructed for the CSW contain reflected and gyrorotating particles (including those in Fig. 6). The temperature T_{i2} exceeds the level determined by adiabatic heating and heating by the ion-acoustic current turbulence. The calculated trajectories of gyrorotating ions inside and behind the terrestrial CSW front do not agree with the actual trajectories (the calculated velocities that are too high).[13] The satellite data were therefore also analyzed with a view to establishing the mechanism of the ion-ion interaction.

An important parameter governing the strength of the ion-ion interaction is the quantity β_i (ratio of thermal ion motion to the magnetic-field pressure ahead of the CSW front).[29] In the laboratory shock waves described above, $\beta_i \ll 1$, but, in space, β_i varies between wide limits, so that the M_A and M_S were normalized to $T_{i\parallel}$, during the analysis of satellite data. Since $\theta_{\mathbf{Vn}}$ is difficult to determine, we used V_{SW} for U in calculations of ζ. Figures 5–8 show the results obtained by analyzing the data given in the above papers in this way.

The increase in the ion temperature ΔT_i in the CSW and the efficiency ζ are decreasing functions of M_A/β_i and M_S/β_i (Figs. 7 and 8). The ratio M_S/β_i increases with in-

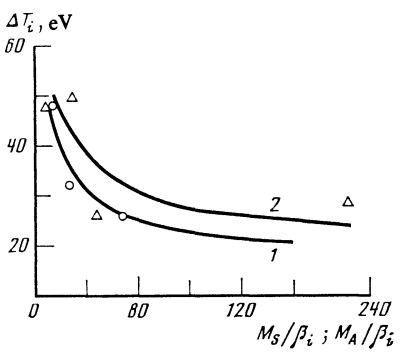

FIG. 7. Increase in ion temperature T_i on a terrestrial CSW front as a function of M_A/β_i (○—curve 1) and M_S/β_i (△—curve 2).

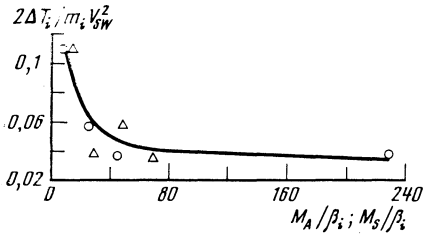

FIG. 8. Efficiency of conversion of the energy of directed motion for a terrestrial a CSW $\zeta = 2\Delta T_i/m_i V_{SW}^2$ as a function of M_A/β_i (△) and M_S/β_i (○).

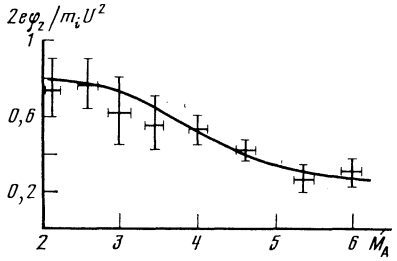

FIG. 9. The quantity $2e\varphi_2/m_i U^2$ as a function of M_A for a laboratory CSW.

creasing M_A/β_i (curve 2, Fig. 5). Figure 6 shows typical proton energy spectra in the region immediately behind the CSW front. Curve 1 corresponds to the maximum values of M_S/β_i and M_A/β_i from among those calculated (data of 27 August 1978, 20:08:00 UT; section along the line of maximum definition of gyrorotating beams of ions; about 7° to the sun-Earth axis; Fig. 12 is from Ref. 13). Two beams of gyrorotating ions are clearly defined behind the CSW front at energies of about 700 and 2200 eV. Curve 2 (7 November 1977, 22:52:13 UT; section along the axis pointing toward the center of the gyrorotating beam lying in the upper half-plane; Fig. 14 is from Ref. 13) was constructed for the minimum values of M_S/β_i, M_A/β_i and has the form of a distribution with a relaxed beam.

In our view, the dominant role of the parameter M_S/β_i is confirmed by the results obtained by the authors of Ref. 26, who measured plasma parameters for the solar wind and the magnetic layer during the pre-Alfven wind. It follows from the graphs given in Fig. 7 of Ref. 26 (p. 243) that the quantity

$$\frac{m_i\langle V^2\rangle}{2} \Big/ \frac{m_i V_{sw}^2}{2}$$

varies during the pre-Alfven solar wind in the range 0.33–0.66, and exceeds the analogous quantity for all the cases mentioned earlier. The number of high-energy particles in the tail of the distribution functions, determined from the energy spectra shown in Fig. 6 of Ref. 26 (p. 243), is of the same order for pre- and post-Alfven wind. Of analogous significance is the fact that the maximum deceleration of the gyroratating ion beam $(V_{b1} - V_d)/V_{b1}$ is observed for small M_S/β_i (V_{b1} is the beam velocity before the CSW front). Moreover, for small M_S/β_i, the actual number of ions reflected by the CSW appears to be greater than the number recorded ahead of the shock wave (1–3%). This is illustrated by the sharp (by approximately two orders) increase as compared with the region before the CSW in the quantity dn_i/dE near E_{refl} on the front of the interplanetary CSW[14] (curves 3 and 4 in Fig. 6). Ions with low M_S/β_i that have been reflected by the CSW are probably rapidly retarded and heat the core of the distribution function as a result.

DISCUSSION OF RESULTS

Reflected particles were observed in the above CSW experiments for all M_A ($1.6 \lesssim M_A \lesssim 6.1$ in the laboratory and $1 \lesssim M_A \lesssim 12$ in space). In an earlier laboratory experiment,[6] the reflection of ions was observed from $M_A \simeq 2.7$ onward, and was related to the approach to M_{c1}. This result may have been a consequence of the low sensitivity of the probe employed and of the magnetic field dependence of the receiving probe aperture. It is interesting in this connection to note the fact that the ratio $2e\varphi_2/m_1U^2$ (which is important for the reflection process) is a maximum for low values of M_A and reaches a value of the order of 0.75 for $M_A \simeq 2$. The increase in M_A leads to a reduction in $2e\varphi_2/m_iU^2$ and, when $M_A \simeq 6$, this ratio becomes $2e\varphi_2/m_iU^2 \simeq 0.25$ (see Fig. 9, which refers to the laboratory CSW).

The temperature T_{i2} was determined in Refs. 3 and 5 from the low-energy part of the ion distribution function averaged over a large number of events in the single-channel energy analyzer and, as noted above, large T_{i2} corresponds to large M_A. The ion signals used to construct the distributions were the resultant signals: we did not resolve bursts of radiation ahead of the CSW and related to its front from the radiation from the piston following the CSW. This was probably the reason why we did not obtain the reduction in T_{i2} with increasing M_A. The increase in T_{i2} was possibly a consequence of the increase in E_{col} with increasing M_A. Thus, for $n_{\text{refl}}/n_0 = 25\%$ (Ref. 13), the energy carried by the reflected ions and acquired during collective interaction becomes comparable with the energy carried by the incident flux.

Terrestrial and laboratory CSW's can evidently be characterized at $t \gg \omega_{Hi}^{-1}$ by the presence of two types of electrostatic wave excited by ion currents moving relative to one another, namely, one in the region of the ion plasma frequency ω_{pi} and the other in the region of the lower hybrid resonance. As M_A increases (at fixed β_i), large-scale oscillations become increasingly important and eventually predominate for strong CSW.[12] The gradual increase in the relative number of reflected particles with increasing M_A (Refs. 6 and 13), and the fact that the jump in the potential for large M_A is only a fraction of the measured change in the ion kinetic energy on reflection (see Fig. 9 and Ref. 30), slow that a fraction of the incident ion current is reflected from the jump in the potential φ_2 ($e\varphi_2 < m_iU^2/2$) as a result of the reduction in the directed velocity during scattering in the region of high oscillation intensity. For experiments with $t \gg \omega_{Hi}^{-1}$, i.e., most laboratory studies, including the present work, the effect of short-wave ion oscillations is dominant.

The ion temperature $\overline{T}_{i2}$ behind the turbulent electrostatic CSW produced in the ion-ion interaction zone between two colliding plasma currents was measured in the experiment described in Ref. 31 as a function of $M_{s1} = U_1/(T_{e1} + 3T_{i1})/m_i)^{1/2}$ (U_1, T_{e1}, T_{i1} are, respectively, the velocity, electron temperature, and ion temperature in the denser plasma flux). The temperature $\overline{T}_{i2}$ was determined from the "averaged" distribution functions (measured in a time $t \gg 2\pi/\omega_{pi}$). The temperature $\overline{T}_{i2}$ was again found to be a decreasing function of M_{S1} under the conditions of predominant heating ($M_{S1} = 1.9$–3.5; Fig. 9 in Ref. 31).

CONCLUSIONS

1. Measurements of the ion temperature T_{i2} behind the CSW front and semiempirical calculations of the electron temperature T_{e2} were used to determine T_{i2} and $\zeta = 2T_{i2}/m_i U^2$ as functions of M_A and M_S. It was found that T_{i2} and ζ decreased with increasing M_A and M_S.

2. Ions reflected by the CSW were recorded at $1.6 \lesssim M_A \lesssim 6.1$. The ion energy distribution function in the region of maximum electron temperature in the shock wave front has the shape of a distribution with a relaxed beam for $M_S \lesssim 3.5$–4 and $M_A \simeq 3$. When $M_S > 3.5$–4, $M_A > 3$, the pure beam-type spectrum persists over the entire front.

3. The dependence of ΔT_i and ζ on M_A, M_S has an analogous character (at fixed β_i) for terrestrial CSW's. The proton energy distribution function also contains a relaxed beam for low M_S, M_A and an intact beam for high values of these parameters.

4. Combined analysis of the results obtained by direct investigation of the ion distribution function in laboratory, terrestrial, and interstellar shock waves leads to the conclusion that the ion-ion interaction in the CSW front produces most of the dissipation of the energy of directed plasma motion by heating the distribution core at low M_S, M_A and by increasing the relative number of reflected ions due to the change in the directed velocity on scattering in the ion-ion interaction zone at high M_S, M_A. As M_S, M_A increase, there is an increase in the total energy received by ions in the collective interaction (the kinetic energy of directed motion of reflected particles plus the thermal energy of the core and beam), and there is an accompanying reduction in T_{i2}.

5. Two short-wave ion-ion instability regimes appear to occur on the CSW front. The value of M_S intermediate between the two regimes, calculated from the change in the shape of the distribution function (plateau → beam) and from the reduction in T_{i2}, is roughly equal to the value of M_S calculated in Ref. 27.

The author is indebted to N. A. Koshilev, A. A. Shishko, and G. N. Kichigin for help and stimulating discussions.

[1]C. F. Kennel and J. P. Edmiston, Preprint PPG-822, Los Angeles, 1984.
[2]S. G. Alikhanov, N. I. Alinovskiĭ, G. G. Dolgov-Savel'ev, V. G. Eselevich, R. Kh. Kurtmullaev, V. I. Malinovskiĭ, Yu. E. Nesterikhin, V. I. Pil'skiĭ, R. Z. Sagdeev, and V. N. Semenov, III Mezhdunarodnaya kongerentsiya po fizike plazmy (Third Intern. Conf. on Plasma Physics), Novosibirsk, 1968, No. CN-24/A-1.
[3]N. I. Alinovskiĭ, V. G. Eselevich, N. A. Koshilev, and R. Kh. Kurtmullaev, Zh. Eksp. Teor. Fiz. **57**, 705 (1969) [Sov. Phys. JETP **30**, 385 (1970)].
[4]W. F. Dove, Phys. Fluids **14**, 2359 (1971).
[5]N. I. Alinovskiĭ, A. T. Altyntsev, and N. A. Koshilev, Zh. Eksp. Teor. Fiz. **62**, 2121 (1972) [Sov. Phys. JETP **35**, 1108 (1972)].
[6]P. E. Phillips and A. E. Robson, Phys. Rev. Lett. **29**, 154 (1972).
[7]T. T. Chiang and A. W. DeSilva, Phys. Fluids **21**, 1053 (1978).
[8]N. A. Koshilev, N. A. Strokin, and A. A. Shishko, Preprint No. 21-84, SibIZMIR SO AN SSSR, Irkutsk, 1984.
[9]J. R. Asbridge, S. J. Bame, and J. B. Strong, J. Geophys. Res. **73**, 5777 (1968).
[10]M. D. Montgomery, J. R. Asbridge, and S. J. Bame, J. Geophys. Res. **75**, 1217 (1970).
[11]E. W. Greenstadt, C. T. Russell, J. T. Gosling, G. Paschmann, G. K. Parks, K. A. Anderson, F. L. Scarf, R. R. Anderson, D. A. Gurnett, C. S. Lin, R. P. Lin, and H. Reme, J. Geophys. Res. **85**, 2124 (1980).
[12]O. L. Vaĭsberg, A. A. Galeev, S. I. Klimov, M. N. Nozdrachev, A. N. Omel'chenko, and R. Z. Sagdeev, Pis'ma Zh. Eksp. Teor. Fiz. **35**, 25 (1982) [JETP Lett. **35**, 30 (1982)].
[13]N. Schopke, G. Paschmann, S. J. Bame, J. T. Gosling, and C. T. Russell, J. Geophys. Res. **88**, 6121 (1983).
[14]J. T. Gosling, S. J. Bame, W. C. Feldman, G. Paschmann, N. Schopke, and C. T. Russell, J. Geophys. Res. **89**, 5409 (1984).
[15]K. Schindler, "Laboratory experiments under simulation of processes occurring in the solar wind and the Earth's magnetosphere," in: The Physics of the Magnetosphere [Russian translation, Mir, Moscow, 1972, p. 66].
[16]C. G. Fälthammar, Space Sci. Rev. **15**, 801 (1974).
[17]I. M. Podgornyĭ and R. Z. Sagdeev, Usp. Fiz. Nauk **98**, 409 (1969) [Sov. Phys. Usp **12**, 445 (1970)].
[18]V. B. Baranov, Kosmicheskie issledovaniya **7**, 109 (1969).
[19]Yu. A. Beresin, R. Kh. Kurtmullaev, and Yu. E. Nesterikhin, Fiz. Goreniya Vzryva **1**, 3 (1966).
[20]V. V. Afrosimov and I. P. Gladkovskiĭ, Zh. Tekh. Fiz. **37**, 1557 (1967) [Sov. Phys. Tech. Phys. **12**, 1135 (1968)].
[21]V. P. Borzenko, N. A. Koshilev, O. G. Parfenov, and N. A. Strokin, Zh. Tekh. Fiz. **48**, 1174 (1978) [Sov. Phys. Tech. Phys. **23**, 655 (1978)].
[22]N. I. Alinovskiĭ, A. T. Altyntsev, and N. A. Koshilev, Zh. Prikl. Mekh. Tekh. Fiz. No. 3, 132 (1970).
[23]A. A. Galeev and R. Z. Sagdeev, Nelineĭnaya teoriya plazmy. V sb. Voprosy teorii plazmy (Nonlinear Plasma Theory, in: Problems in Plasma Theory), Atomizdat, Moscow, 1973, No. 7, p. 119.
[24]M. P. Berezovskiĭ, I. V. Petrov, I. K. Konkashbaev, and A. M. Rubenchik, Dokl. Akad. Nauk SSSR **268**, 1369 (1983) [Sov. Phys. Dokl. **28**, 169 (1983)].
[25]A. L. Chernyakov, Fiz. Plazmy **7**, 573 (1981) [Sov. J. Plasma Phys. **7**, 311 (1981)].
[26]J. T. Gosling, J. R. Asbridge, S. J. Bame, W. C. Feldman, R. D. Zwickl, G. Paschmann, N. Schopke, and C. T. Russell, J. Geophys. Res. **87**, 239 (1982).
[27]A. A. Ivanov, S. I. Krasheninnikov, T. K. Soboleva, and P. N. Yushmanov, Fiz. Plazmy **1**, 753 (1975) [Sov. J. Plasma Phys. **1**, 412 (1975)].
[28]E. Marsch, K. H. Mühlhäuser, R. Schwenn, H. Rosenbauer, W. Pilipp, and F. M. Neubauer, J. Geophys. Res. **87**, 52 (1982).
[29]P. C. Liewer, Nucl. Fusion **16**, 817 (1976).
[30]V. Formisano, Geophys. Res. Lett. **9**, 1033 (1982).
[31]V. G. Eselevich and V. G. Faĭnshteĭn, Fiz. Plazmy **10**, 538 (1984) [Sov. J. Plasma Phys. **10**, 313 (1984)].
[32]R. Kh. Kurtmullaev, V. I. Pil'skiĭ, and V. N. Semenov, Zh. Tekh. Fiz. **40**, 1044 (1970) [Sov. Phys. Tech. Phys. **15**, 804 (1970)].

Translated by S. Chomet